Full Matlab Code for Synthesis and Optimization of Bragg Gratings

Full Matlab Code for Synthesis and Optimization of Bragg Gratings

By

Fethallah Karim

TABLE OF CONTENTS

I.

INTRODUCTION

The use of new optical fiber devices in the telecommunication sector has seen an important development in the last few years. Among them, Fiber Bragg Gratings (FBG) based devices represent an attractive and cheap alternative for applications such as multichannel filtering, multichannel optical add/drop multiplexing, multichannel dispersion compensation and multi wave length laser sources.

The fiber Bragg grating is a periodic variation of the refractive index along the propagation direction in the core of the fiber. It can be fabricated by exposing the core of the optical fiber to UV radiations. This induces the refractive index change along the core of the fiber.

The coupled mode theory is most widely used to analyze light propagation in a weakly coupled waveguide medium. The fiber Bragg grating is a weakly coupled waveguide structure [1]. The coupled mode equations that describe the light propagation in the grating can be obtained by using the coupled mode theory. There are no analytical solutions for these coupled mode equations as yet. Numerical methods must be used to solve these equations.

The transfer matrix method and the direct numerical integration method have been used to calculate the solution of the coupled-mode equations. Several techniques have been used to fabricate the fiber Bragg gratings: the phase mask technique, the point-by-point technique and the interferometric technique [2].

Uniform Bragg gratings cannot satisfy the demand of some kind of applications alone. New types of grating are being manufactured and studied by researchers. The chirped, apodized and sampled Bragg gratings are some examples of modified gratings that will be studied and simulated in this work.

Controlling, combining and routing light are the three main uses of fiber Bragg gratings in optical communications. For combining the light, fiber Bragg gratings can be used to combine different wavelengths on a single optical fiber [3]. This feature of fiber Bragg gratings can be used in wavelength division multiplexing (WDM) systems. Different wavelengths can be added or dropped in a WDM system by using the route feature of the fiber Bragg grating [4].

At the end of this document, some channels densification techniques will be presented in a case of mono canal and multi channel gratings, these channels can be shifted to desired wavelengths by applying temperature and strain constraints.

II.

THEORY AND FUNDAMENTALS OF FIBER BRAGG GRATINGS

II.1 Introduction

In 1978, at the Canadian Communications Research Center (CRC), Ottawa, Ontario, Canada [5], K.O. Hill *et al* first demonstrated the refractive index changes in a germano-silica optical fiber by launching a beam of intense light into a fiber. In 1989, a new writing technology for fiber Bragg gratings, the ultraviolet (UV) light side-written technology, was demonstrated by Meltz *et al* [6]. Since then, much research has been done to improve the quality and durability of fiber Bragg gratings. Fiber gratings are the keys to modern optical fiber communications and sensor systems. The commercial products of fiber Bragg gratings have been available since early 1995.
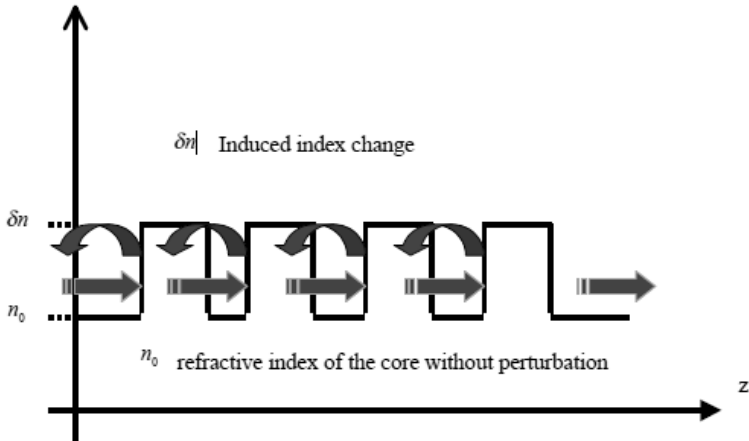
Fig (1). Refractive index change of the fiber Bragg grating [1]

A fiber Bragg grating is a periodic perturbation structure of the refractive index in a waveguide. Fiber gratings can be manufactured by exposing the core of a single mode communication fiber to a periodic pattern of intense UV light. The exposure induces a permanent refractive index change in the core of the fiber. This fixed index modulation depends on the exposure pattern [II.1]. Figure (1) shows the periodic change in the refractive index of the fiber core. This short length optical fiber with the refractive index modulation is called a fiber Bragg grating.

The Refractive index modulation can be represented by [7]

$$n(x, y, z) = \overset{\rho}{n}(x, y, z) + \delta n(x, y, z) \cos\left(\frac{2\pi}{\Lambda} z\right) \qquad (1)$$

where $\overset{\rho}{n}(x, y, z)$ is the average refractive index of the core, $\delta n(x, y, z)$ is the modulation of the refractive index, and Λ is the Bragg period.

A small amount of incident light is reflected at each periodic refractive index change. The entire reflected light waves are combined into one large reflection at a particular wavelength when the strongest mode coupling occurs. This is referred to as the Bragg condition (2), and the wavelength at which this reflection occurs is called the Bragg wavelength. Only those wavelengths that satisfy the Bragg condition are affected and strongly reflected. The reflectivity of the input light reaches a peak at the Bragg wavelength. The Bragg grating is essentially transparent for an incident light at wavelengths other than the Bragg wavelength where phase matching of the incident and reflected beams occurs [P.1]. The Bragg wavelength λ_B is given by [P.2], as follows:

$$\lambda_B = 2n_{eff}\Lambda \qquad (2)$$
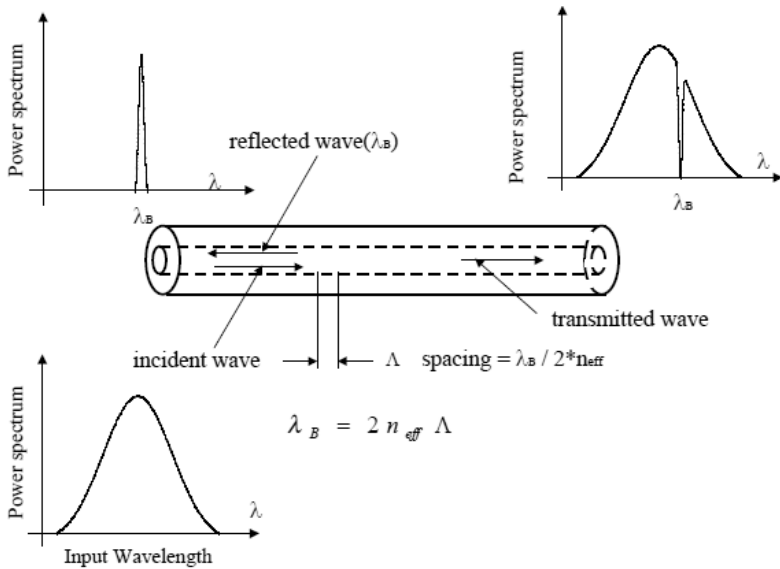
Fig (2). Diagram illustrating the properties of the fiber Bragg grating [1]

where n_{eff} is the effective refractive index and Λ is the grating period. This is the condition for the Bragg resonance. From equation (2), we can see that the Bragg wavelength depends on the refractive index and the grating period.

Long gratings with a small refractive index excursion have a high peak reflectance and a narrow bandwidth, as can be seen on Fig (2).

The fiber Bragg grating has the advantages of a simple structure, a low insertion loss, a high wavelength selectivity, a polarization insensitivity and a full compatibility with general single mode communication optical fibers. Uniform Bragg gratings are basically a reflectance filters. According to an application, they can have bandwidths of less than 0.1nm. It is also possible to make a wide bandwidth filter that is tens of nanometres wide. Reflectivity at the Bragg wavelength can also be designed to be as low as 1% or greater than 99.9%. Fiber grating characteristics such as photosensitization, apodization, dispersion, bandwidth control, temperature constraint, strain responses, thermal compensation and reliability issues have been used in optical communications and sensor systems [8].

II.2 Coupled mode theory

In general, we are interested in the spectral response of the Bragg grating. The characteristics of the fiber Bragg grating spectrum can be understood and modelled by several approaches. The most widely used theory is the coupled mode theory [9],[10]. The coupled-mode theory is a suitable tool to describe the propagation of the optical waves in a waveguide with a slowly varying index along the length of the waveguide. Fiber Bragg gratings have this type of structure. The basic idea of the coupled-mode theory is that the electrical field of the waveguide with a perturbation can be represented by a linear combination of the modes of the field distribution without perturbations [P.2].

The modal fields of the fiber can be represented by [II.1]

$$E_{\pm j}(x, y, z) = e_{\pm j}(x, y) \times \exp(\pm i\beta_j z) \quad j=1,2,3,\ldots \qquad (3)$$

where $e_{\pm j}(x, y)$ is the amplitude of the transverse electric field of the jth propagation mode and $\pm$ represents the propagation direction, and β_j is called the propagation constant or eigenvalue of the jth mode. Generally, each mode has a unique value of β_j. In this work, we implicitly assume a time dependence $\exp(-iwt)$ for the fields where w is the angular frequency. The propagation of the light along the optical waveguides in the fiber can be described by the Maxwell's equations. Propagation modes are the solutions of the source-free Maxwell equation [9].

In terms of the coupled-mode theory, the transverse component of the electric field at the position z in the perturbed fiber can be described by a linear superposition of the ideal guided modes of the unperturbed fiber, which can be written as [P.2]

$$\vec{E}_t(x, y, z, t) = \sum_j \left[E_j(x, y, z, t) + E_{-j}(x, y, z, t) \right] \qquad (4)$$

Be substituting the modal field equation (3) into (4), the electric field $\vec{E}_t(x, y, z, t)$ can be written as [II.1]

$$\vec{E}_t(x, y, z, t) = \sum_j \left[A_j^+(z) \exp(i\beta_j z) + A_j^-(z) \exp(-i\beta_j z) \right] \times \vec{e}_{jt}(x, y) \exp(-iwt) \qquad (5)$$

where $A_j^+(z)+$ and $A_j^-(z)$ are slowly varying amplitudes of the jth forward and backward travelling waves respectively; β_j is the propagation constant; and $\vec{e}_{jt}(x,y)$ is the transverse mode field. This electric field distribution $\vec{E}_t(x,y,z,t)$ can be solved by modal methods. $\vec{E}_t(x,y,z,t)$ is one of the solutions of Maxwell's equation.

The index of the grating is z-dependent along the fiber. The refractive index $n(x,y,z)$ in equation (1) can be rewritten as [P.1]

$$n(x,y,z) = n(z) = n_0 + \delta n_0 + \delta n(z)\cos\left(\frac{2\pi}{\Lambda}z + \varphi(z)\right) \qquad (6)$$

where the average refractive index $\overline{n}$ is represented as $n_0 + \delta n_0$, and $n_0 \gg \delta n_0$; n_0 is the refractive index of the core without the perturbation; δn_0 is the average index modulation (DC change); $\delta n(z)$ is the small amplitude of the index modulation (AC change); $\varphi(z)$ is the phase of the grating; and Λ is the Bragg period.

The electric field distribution in the grating, $\vec{E}_t(x,y,z,t)$ satisfies the scalar wave propagation equation. This follows from a simplification of the Maxwell's equations under the weak propagation approximation, and is given by [1]

$$\left[\nabla_t^2 + k^2 n^2(x,y,z) - \beta^2\right]\vec{E}_t(x,y,z,t) = 0 \qquad (7)$$

where $k = \dfrac{2\pi}{\lambda}$ is the free space propagation constant, and λ is the free space wavelength.

The electric field $\vec{E}_t(x,y,z,t)$ and the refractive index $n(x,y,z)$ are substituted into the wave propagation equation (7) to yield the following coupled-mode equations [II.1]

$$\frac{dA_n^+}{dz} = i\sum_m A_m^+ \left(K_{mn}^t + K_{mn}^z\right)\exp[i(\beta_m - \beta_n)z] + i\sum_m A_m^- \left(K_{mn}^t - K_{mn}^z\right)\exp[-i(\beta_m + \beta_n)z] \quad (8)$$

$$\frac{dA_n^-}{dz} = -i\sum_m A_m^+ \left(K_{mn}^t - K_{mn}^z\right)\exp[i(\beta_m + \beta_n)z] - i\sum_m A_m^- \left(K_{mn}^t + K_{mn}^z\right)\exp[-i(\beta_m - \beta_n)z] \quad (9)$$

where $K_{mn}^t(z)$ is the transverse coupling coefficient between modes n and m, $K_{mn}^t(z)$ is given by [10]

$$K_{mn}^t(z) = \frac{w}{4}\iint\limits_\infty dxdy\,\Delta\varepsilon(x,y,z)\vec{e}_{mt}(x,y)\vec{e}_{mt}^*(x,y) \quad (10)$$

where $\Delta\varepsilon$ is the perturbation to the permittivity. Under the weak waveguide approximation ($n_0 \gg \delta n_0$), $\Delta\varepsilon \cong 2n\delta n$. In general, $K_{mn}^z \ll K_{mn}^t$ for fiber modes, and this coefficient is thus usually neglected.

II.3 Applications of fiber Bragg grating

Table I. Applications of fiber Bragg gratings

Fiber grating sensors
Temperature, strain and pressure sensors [11] [12]
Distributed fiber Bragg grating sensor systems [13]
Fiber lasers
Fiber grating semiconductor lasers [14]
Stabilization of external cavity semiconductor lasers [15]
Erbium-doped fiber lasers [16]
Fiber optical commnications
Dispersion compensation [17]
Wavelength division multiplexed networks [18]
Gain flattening for erbium-doped fiber amplifiers [19]
Add/Drop multiplexers [20]
Comb filters [21]
Interference reflectors [13]
Pulse compression [22]
Wavelength tuning [23]
Raman amplifiers [24]
Chirped pulse amplification [25]

There are a number of applications of fiber gratings in lasers, communications and sensors. For example, fiber Bragg gratings can be used as a multiplexer and a demultiplexer in wavelength division multiplexed systems, and as a dispersion compensator in communication systems (see table I).

Fiber Bragg gratings have a low insertion loss, a low polarization-dependent loss and an excellent spectral response profile. This makes them suitable for the applications of fiber optical sensors [10].

They can be used for the manufacturing of the fiber lasers on the device manufacturing [1].

II.4 Modeling of fiber Bragg grating

In most fiber gratings, the induced index change is approximately uniform across the core, and there are no propagation modes outside the core of the fiber. In terms of this supposition, the cladding modes in the

fiber are neglected in this simulation program. If we neglect the cladding modes, the electric field of the grating can be simplified only to the superposition of the forward and backward fundamental mode in the core. The electric field distribution (4) along the core of the fiber can be expressed in terms of two counter-propagating modes under the two-mode approximation [9].

$$E(x, y, z, t) = \left[A_j^+(z) \exp(-i\beta_j z) + A_j^-(z) \exp(i\beta_j z) \right] \times e_t(x, y) \quad (11)$$

where $A+$ (z) and $A-$ (z) are slowly varying amplitudes of the forward and backward travelling waves along the core of the fiber, respectively. The term $E(x, y, z)$ from equation (4) can be substituted into coupled-mode equations (8) and (9). The coupled-mode equations can be simplified into two modes, which are described as [9]

$$\frac{dR(z)}{dz} = i\hat{\sigma}(z)R(z) + ik(z)S(z) \quad\quad (12)$$

$$\frac{dS(z)}{dz} = -i\hat{\sigma}(z)S(z) - ik(z) * S(z) \quad\quad (13)$$

where $R(z) = A^+(z) \exp\left[i\left(\delta z - \frac{\phi}{2} \right) \right]$ and $S(z) = A^-(z) \exp\left[-i\left(\delta z - \frac{\phi}{2} \right) \right]$ [26]; $R(z)$ is the forward mode and $S(z)$ is the reverse mode, and they represent slowly varying mode envelope functions. $\hat{\sigma}$ is a general "DC" self-coupling coefficient [10], and $k(z)$ is the "AC" coupling coefficient [10], also called the local grating length [27].

The simplified coupled-mode equations (12) and (13) are used in the simulation of the spectral response of the Bragg grating. The coupling coefficient $k(z)$ and the local detuning $\hat{\sigma}(z)$ are two important parameters in the coupled mode equations (12) and (13). They are fundamental parameters in the calculation of the spectral response of the fiber Bragg gratings. The notations of these two parameters are different, depending on the different authors in the literature.

The general "DC" self-coupling coefficient $\hat{\sigma}$ can be represented by [1]

$$\delta\!\!\!/ = \delta + \frac{2\pi}{\lambda}\delta n_{eff} - \frac{1}{2}\frac{d\phi}{dz} \tag{14}$$

Where $\frac{1}{2}\frac{d\phi}{dz}$ is describing a possible chirp of the grating period, and ϕ is the grating phase [10]. The detuning δ can be represented by [P1]

$$\delta = \beta - \frac{\pi}{\Lambda}$$

$$= \beta - \beta_D \tag{15}$$

$$\delta = 2\pi n_{eff}\left(\frac{1}{\lambda} - \frac{1}{\lambda_D}\right)$$

where $\lambda_D = 2n_{eff}\Lambda$ is the design wavelength for the Bragg reflectance and δn_{eff} is the refractive index change.

The coupling coefficient $k(z)$ can be represented by [P1]

$$k(z) = \frac{\pi}{\lambda}\delta n_{eff}\,g(z)v \tag{16}$$

where $g(z)$ is the apodization function and v is fringe visibility.

There is no input signal that is incident from the right-hand side of the grating S(+L/2)=0 , and there is some known signal that is incident from the left side of the grating R(-L/2)=1 (**fig (3)**). Depending on these two boundary conditions, the initial condition of the grating can be written as in equations (17) and (18). The reflection and transmission coefficients of the grating can be derived from the initial conditions and the coupled-mode equations.
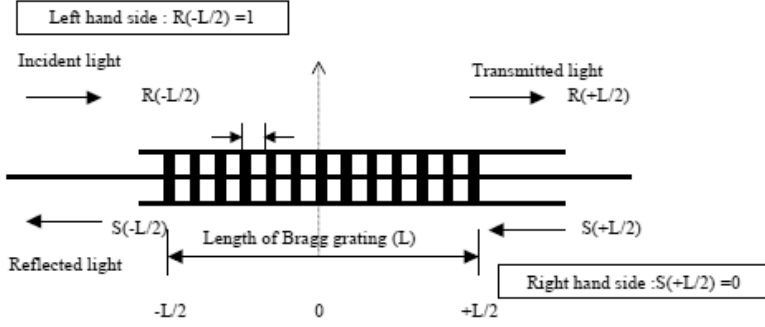
Fig (3). The initial condition and calculation of the grating response to input field [1]

Left side :

$$\left\{ \begin{array}{l} S\left(-\dfrac{L}{2}\right) = ? \\[4mm] R\left(\dfrac{-L}{2}\right) = 1 \end{array} \right\} \tag{17}$$

Right side :

$$\left\{ \begin{array}{l} R\left(+\dfrac{L}{2}\right) = ? \\[4mm] S\left(\dfrac{+L}{2}\right) = 0 \end{array} \right\} \tag{18}$$

The amplitude of the reflection coefficient ρ can be written as

$$\rho = \frac{S\left(-\dfrac{L}{2}\right)}{R\left(-\dfrac{L}{2}\right)} \tag{19}$$

The power reflection coefficient *r* (reflectivity) can be written by

$$r = \left| \rho^2 \right| \tag{20}$$

II.5 Uniform Bragg grating

The phase matching and the coupling coefficient are constant in the case of uniform Bragg gratings. Equations (12) and (13) are first-order ordinary differential equations with constant coefficients. There are analytical solutions for equations (2) and (3). The analytical solutions of the coupled-mode equations can be found with the boundary conditions from equations (17) and (18).

As the chirp $\dfrac{d\phi}{dz}$ is zero, the local detuning $\hat{\sigma}$ is described as:

$$\hat{\sigma} = \delta + \frac{2\pi}{\lambda}\delta n_{eff} \quad (21)$$

The solution of the complex reflection and transmission coefficients can be expressed by [29]

$$A^-(z) = \frac{-ik \sinh\left[\gamma_B\left(z - \dfrac{L}{2}\right)\right]}{i\hat{\sigma}\sinh(\gamma_B L) + \gamma_B \cosh(\gamma_B L)} \tag{22}$$

$$A^+(z) = \frac{\gamma_B \cosh\left[\gamma_B\left(z - \dfrac{L}{2}\right)\right] - i\hat{\sigma}\sinh\left(\gamma_B\left(z - \dfrac{L}{2}\right)\right)}{i\hat{\sigma}\sinh(\gamma_B L) + \gamma_B \cosh(\gamma_B L)} \tag{23}$$

where γ_B is described by [29]

$$\gamma_B = \sqrt{k^2 - \hat{\sigma}^2}\left(k^2 > \hat{\sigma}^2\right) \tag{24}$$

$$\gamma_B = i\sqrt{\hat{\sigma}^2 - k^2}\left(k^2 < \hat{\sigma}^2\right) \tag{25}$$

The reflected spectrum can be obtained and described by [29]

$$r(\lambda) = \frac{k^2 \sinh^2(\gamma_B L)}{\hat{\sigma}^2 \sinh^2(\gamma_B L) + \gamma_B^2 \cosh^2(\gamma_B L)} \tag{26}$$

The phase of the reflected light with respect to the incident light can be obtained from equations (22) and (23), and is described by [28]

$$\Phi(\lambda) = \tan^{-1}\left[\frac{\gamma_B}{\hat{\sigma}} \coth(\gamma_B L)\right] \tag{27}$$

At the Bragg wavelength, $\hat{\sigma} = 0$, the grating has the peak reflectivity r_{max}, which is [28]

$$r_{max} = r(\lambda_D) = \tanh^2(|k|L) \tag{28}$$

It is evident from equation (28) that the reflectivity of Bragg gratings is close to 1 when the modulation of the index and the grating length are increased.

The group time delay and the dispersion of the grating can be obtained from the phase information $\Phi(\lambda)$ of the reflection coefficient [P1].

The delay time τ_p (in ps) for the reflected light in a grating is defined as follows [P1]

$$\tau_p = \frac{d\Phi}{dw} = -\frac{\lambda^2}{2\pi c}\frac{d\Phi}{d\lambda} \tag{29}$$

The dispersion d_p (in ps/nm) can be defined as [P1]

$$d_p = \frac{d\tau_p}{d\lambda} = \frac{2\tau_p}{\lambda} - \frac{\lambda^2}{2\pi c} \frac{d^2\theta_p}{d\lambda^2}$$

$$d_p = -\frac{2\pi c}{\lambda^2} \frac{d^2\theta_p}{dw^2}$$

(30)

II.6 The transfer Matrix method for the Bragg grating simulation

The transfer matrix method was first used by Yamada [30] to analyze optical waveguides. This method can also be used to analyze the fiber Bragg problem. The coupled-mode equations (12) and (13) can be solved by the transfer matrix method for both uniform and non-uniform gratings. Figure (2.4(a)) is the basic ideal structure that the transfer matrix
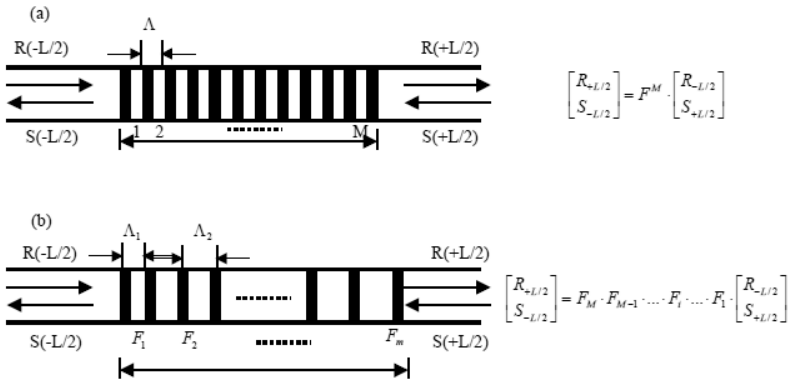
Fig (4). The principle diagram of the transfer matrix method (a) uniform grating (b) non-uniform grating [1]

method uses to solve for a uniform Bragg grating. The refractive index excursion and the period remain constant. For this case, the 2 x 2 transfer matrix is identical for each period of the grating. The total transfer matrix is obtained by multiplying the individual transfer matrices.

A non-uniform fiber Bragg grating can be divided into many uniform sections along the fiber. The incident lightwave propagates through each

uniform section *i* that is described by a transfer matrix F_i . For the structure of the fiber Bragg grating, the matrix F_i can be described as [10]

$$F_i = \begin{bmatrix} \cosh(\gamma_B dz) - i\dfrac{\hat{\sigma}}{\gamma_B}\sinh(\gamma_B dz) & -i\dfrac{k}{\gamma_B}\sinh(\gamma_B dz) \\ i\dfrac{\hat{\sigma}}{\gamma_B}\sinh(\gamma_B dz) & \cosh(\gamma_B dz) + i\dfrac{\hat{\sigma}}{\gamma_B}\sinh(\gamma_B dz) \end{bmatrix} \tag{31}$$

where *k* is described by the equation (16), $\hat{\sigma}$ is described by the equation (14) and γ_B is described by equations (24) and (25).

The entire grating can be represented by [1]

$$\begin{bmatrix} R_{+L/2} \\ S_{-L/2} \end{bmatrix} = F_M \times F_{M-1} \times \ldots\ldots \times F_i \times \ldots\ldots \times F_1 \times \begin{bmatrix} R_{-L/2} \\ S_{+L/2} \end{bmatrix} \tag{32}$$

II.7 Chirped fiber Bragg gratings

II.7.1 The principle of a chirped Bragg grating

A chirped Bragg grating is a grating that has a varying grating period. There are two variables that can be changed to obtain a chirped grating from the equation (2): one is to change the Bragg period; another is to change the refractive index along the propagation direction of the fiber [P1].

Short Wavelengths -------►   Long Wavelengths
(Higher Frequencies)   (Lower Frequencies)
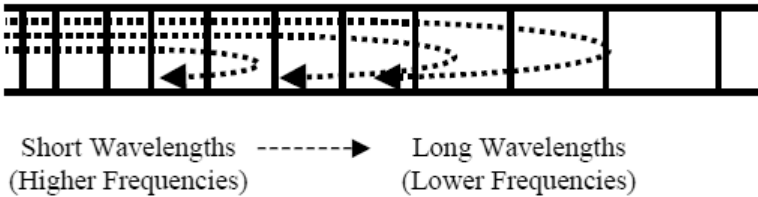
Fig (5). A linear chirped Bragg grating [1]

Figure (5) shows a linear chirped Bragg grating. In this case, the period of the grating varies linearly with the position. This makes the grating

reflects different wavelengths (or frequencies) at different points along its length [1].

Chirped Bragg gratings can also be modeled by the coupled-mode theory. The refractive index of the chirped Bragg grating can be expressed by [10]

$$n(x,y,z) = \overset{\rho}{h}(x,y,z) + \delta n(x,y,z)\cos\left(\frac{2\pi z}{\Lambda} + 2\int_0^z \phi(\xi)d\xi\right) \quad (33)$$

where Λ is the Bragg period and $\phi(\xi)$ describes the instantaneous phase of the chirped grating. There are no analytical solutions for the coupled-mode equations of chirped gratings. Numerical methods must be used to solve the equations.

The period is changed along the z-direction, so that the Bragg wavelength λ_B of any point is different in the Bragg grating.

Changing the refractive index δn along the z-direction has the same effect as changing the period along the z-direction. This means that the optical period is changed even though the physical period of the grating is fixed. So, these two variables can be merged, and described by one variable.

The phase term $\dfrac{1}{2}\dfrac{d\phi}{dz}$ in equation (14) is related to a physical or an optical period change, it can be written as [P3] [P1]

$$\frac{1}{2}\frac{d\phi_{physical}}{dz} = \frac{\pi}{\Lambda(z)} \quad (34)$$

$$\frac{1}{2}\frac{d\phi_{optical}}{dz} = \frac{4\pi \times n_{eff} \times b(i)}{\lambda_D^2} \times \frac{d\lambda_D}{db} \quad (35)$$

$$\frac{1}{2}\frac{d\phi_{optical}}{dz} = F \times \frac{b(i)}{L^2} \quad (36)$$

where $\Lambda(z)$ is the physical period, it can be written as [P3]

$$\Lambda(z) = \Lambda_0 + c_g \qquad (37)$$

Λ_0 is the initial physical period and c_g is the grating chirp parameter.

n_{eff} is the effective refractive index, $\dfrac{d\lambda_D}{db}$ is a rate of a change of the design wavelength with the position in the grating (chirp variable) , F is the chirp parameter and L is the grating length.

Both the chirp variable $\dfrac{d\lambda_D}{db}$ and the chirp parameter F can be used to solve the coupled mode equations of the linear chirped grating.

The parameter $b(i)$ represents the refractive index chirp distribution at each section of the grating, it can be written as [P4]

$$b(i) = c_{g1}(i - 1), \text{ i=1....N} \qquad (38)$$

b, initialized to zero at the first section, increases by the chirp c_{g1} until it reaches the maximum refractive index change chirp at the end of the Bragg grating, while N is the number of sections.

In order to make an equivalence between the physical period chirp c_g , the refractive index chirp c_{g1} and the chirp variable $\dfrac{d\lambda_D}{db}$, we have synthesized the optical period chirp (refractive index chirp c_{g1} and the chirp variable) from the physical period chirp (c_g).

Table II. Bragg gratings parameters used for simulation

Grating parameters	Figure (6)	Figure (7)	Figure (8)	Figure (9)
Grating length (L (cm))	0.7	0.5	1 0.7 0.5	0.7
Refracrive index change (δn)	0.0004	0.0004	0.0004	0.0002 0.0004 0.0006
Effective index refraction (n_{eff})	1.447	1.447	1.447	1.447
Bragg wavelength (λ_D (μm))	1.550	1.550	1.550	1.550
Chirp variable ($d\lambda_D/db$(nm/cm))	-1 +1	-1 -2 -4	-1	-1
Maximum refractive index chirp (b(i))	0.7	0.7	0.7	0.7
Number of sections (N)	150	150	150	150

We assume that the initial physical period Λ_0 is 535.6 nm and the physical chirp c_g is 0.0335 nm, the reconstructed refractive index chirp c_{g1} and the chirp variable $\dfrac{d\lambda_D}{db}$ values are 0.0337 and -1.3821 nm/cm, respectively.

II.7.2 The simulation results of the spectral response

Linear chirped Bragg gratings can be simulated by the simulation program developed in this work. We can use this simulation to optimize the design of the chirped Bragg gratings. Table II summarizes the Bragg grating parameters used in these simulations.

II.7.2.1 Linear chirped gratings with different chirp variables

The first simulation of linear chirped gratings is presented for two gratings with the same parameters. Only the sign of the chirp variable $d\lambda_D/dz$ is reversed.

Figure (6) contains the simulation results of the reflectance with a changed chirp variable $d\lambda_D/dz$. The refractive index δn and the grating length L are fixed. If $\dfrac{d\lambda_D}{db}$ is positive, the period of the linear chirped grating increases along the propagation direction. On the other hand, if $\dfrac{d\lambda_D}{db}$ is negative, the period of the linear chirped grating reduces along the propagation direction. In the simulation program, the value of $\dfrac{d\lambda_D}{db}$ can be positive or negative. In the plot of Fig (6), we can see that the spectral responses of these two linear chirped gratings are shifted from the designed Bragg wavelength.
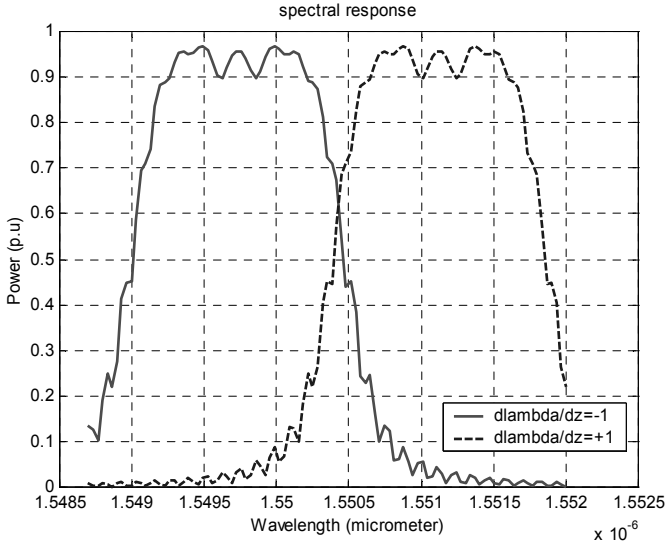
Fig (6). The reflectivity spectrum of two chirped gratings, with an equal chirp with different signs [P1]

If $\dfrac{d\lambda_D}{db}$ is negative, the centre wavelength of the grating moves to the left

hand side (shorter λ). If $\dfrac{d\lambda_D}{db}$ is positive, the centre wavelength of the

grating moves to the right hand side (longer λ). Both of them have the same 3 dB bandwidth.

Figure (7) shows that the 3dB bandwidth of the reflectance spectrum is

increased when the value of the chirp variable $\dfrac{d\lambda_D}{db}$ is increased, whereas

the reflectance is reduced. This is not what we expected intuitively. So we can see that the increased bandwidth results in the reduced reflectance at the same time. Figure (7) shows also that the centre wavelength is shifted with different values of the chirp variable. This feature can be utilized in sensor systems [II.1].

II.7.2.2 Linear chirped gratings with different lengths

Figure (8) shows the reflectance spectrum of linear chirped gratings with different lengths where the chirp variable $d\lambda_D/dz$ is the same.

In Figure (8), we used the same value of the chirp variable $\dfrac{d\lambda_D}{db}$ in the

simulation. The maximum reflectance is almost the same whereas the length of the chirped grating is increased. The bandwidth increase is proportional to the length.
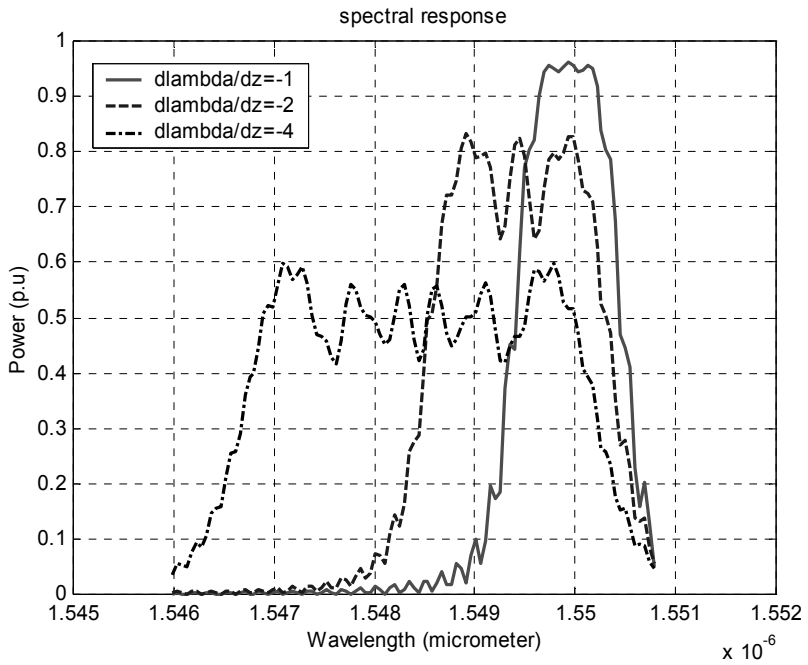
(a)

Fig (7). The reflectivity spectrum of two chirped gratings, with different values of the chirp variable [P4]
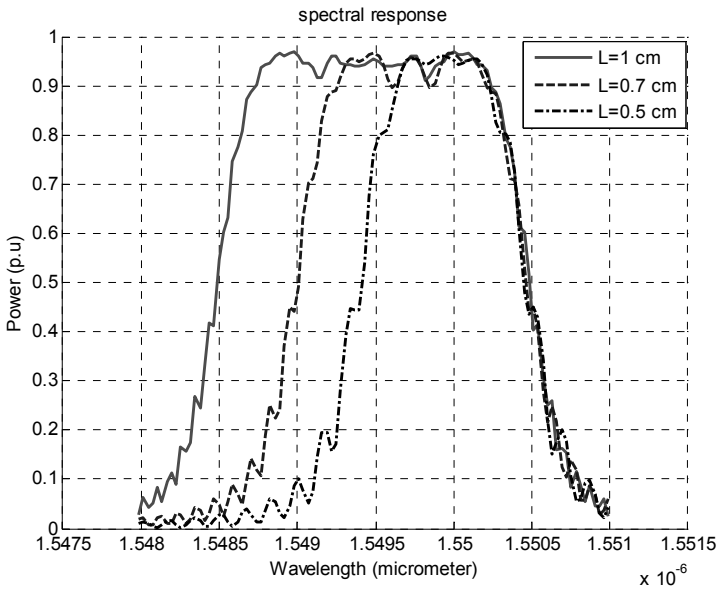
Fig (8). The reflectivity spectrum of three chirped gratings, with different lengths [P1]

II.7.2.3 Linear chirped gratings with different refractive index change

Figure (9) shows the reflectance spectrum of linear chirped gratings with different values of the refractive index change δn.
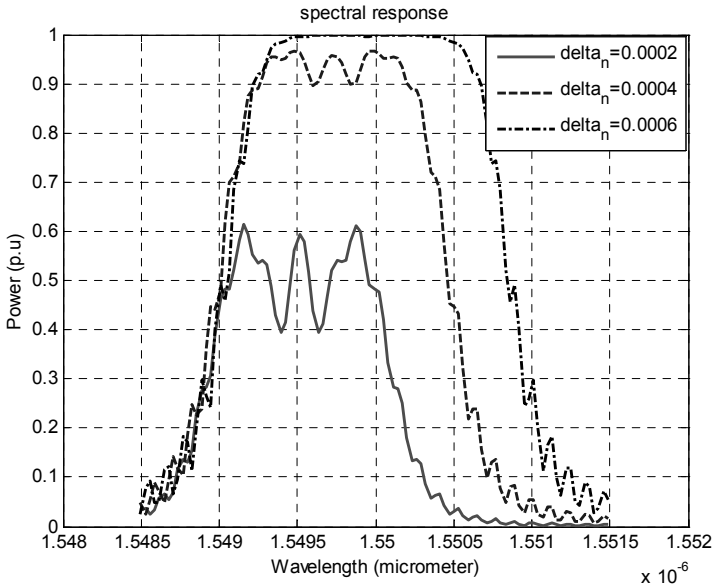
Fig (9). The reflectivity spectrum of three chirped grating with different refractive index change [P1]

The reflectance is increased with increasing δn values. At the same time, the 3dB bandwidth of the reflectance is increased slightly. In this simulation, the value of the chirp variable $\dfrac{d\lambda_D}{db}$ is kept constant. The increase in the index value δn is limited by the fabrication technology used for the grating. The index change δn can only be changed in certain limited range. A flat reflectance spectrum can also be obtained by increasing the length of the grating as shown in fig (8).

II.7.2.4 The Relationship between the centre wavelength and the chirped grating coefficients

The centre wavelength is an important variable in the chirped Bragg grating. It is dependent on the chirp parameter or the chirp variable, the refractive index change and the grating length. The simulation results will show the relationship between the centre wavelength and the chirped grating coefficient.